International Journal of Applied Mathematics
Volume 38 No. 12s 2025,
ISSN: 1311-1728 (printed version); ISSN: 1314-8060 (on-line version)

A BRAIN-CONNECTED NETWORK MODEL - ACQUIRING MRI STRUCTURAL AND FUNCTIONAL CHARACTERISTICS TO ENHANCE ALZHEIMER'S DISEASE PREDICTION

[1]S. Karpagam, [2]Dr. B. Rosiline Jeetha
[1]Research Scholar
Department of Computer Science
Dr.N.G.P.Arts and Science College
Coimbatore- 641048, Tamilnadu, India
karpagam26may@gmail.com
2Professor and Head – Computer Science with AI
Nirmala College for Women
Coimbatore-641018, Tamilnadu, India
Jeethasekar@gmail.com

ABSTRACT

Alzheimer's disease (AD) is a progressive neurodegenerative disorder that steadily deteriorates brain structure and function, ultimately leading to a significant decline in cognitive abilities. Timely diagnosis may stop disease development and improve patient outcomes, making early detection of AD critical. For a correct diagnosis of AD, Magnetic Resonance Imaging (MRI) is crucial. On the other hand, imaging methods necessitate better training and more time. Automated and precise AD detection has recently been made possible with the help of Deep Learning (DL) methods. These methods are able to learn intricate patterns from massive amounts of imaging data, picking up on small variations that people would detect. Yet, many existing DL methods focus primarily on single-modality data or shape-based features, often neglecting other complementary information. As a result, they fail to fully capture the complex interactions within the brain, leading to reduced classification performance. This research suggests a new multimodal framework, Enhanced Ensemble Brain Connected Alzheimer's Disease Network (EEBCADnet), which integrates physical along with functional MRI data, to circumvent this shortcoming. To create 360 ROIs, the suggested approach mostly uses fMRI data that has been preprocessed along with parcellated utilizing the Glasser atlas. Then, Functional connectivity (FC) matrices are constructed by computing correlations among ROI time series, followed by graph-theoretical feature extraction to capture both local and global network measures. To combine these functional features with structural features, a concatenation strategy is employed which forms a fused feature vector. A fully connected (FC) layer as well as a softmax layer are used to make the final stage-wise AD forecast using these vectors. Experimental results on the ADNI and OASIS-3 datasets show that EEBCADnet consistently outperforms traditional models—including CNN, SVM-ANN, 2DCNN-SVM, CSEPC, and MAGNet, achieving accuracies of 93.58% and 94.23%, respectively. The suggested method is robust and reliable, and paired t-test analysis proves that these enhancements are statistically significant.

Keywords: AD, sMRI, fMRI, Feature Extraction, DL

Received: August 04, 2025

International Journal of Applied Mathematics
Volume 38 No. 12s 2025,
ISSN: 1311-1728 (printed version); ISSN: 1314-8060 (on-line version)

1. INTRODUCTION

The most common type of dementia, AD, is a neurodegenerative disease that develops over time and results in neuronal damage and cognitive loss due to the accumulation of β-amyloid plaques and neurofibrillary tangles in the brain [1]. According to the World Health Organization, dementia is one of the primary causes of impairment in the elderly and the sixth leading cause of death worldwide [2]. Brain areas crucial to memory formation (the hippocampus), spatial navigation (the entorhinal cortex) and higher-level cognitive processes (the cerebral cortex) (e.g., language and reasoning) are most severely affected by the disease [3]. Memory loss, poor cognition, behavioral or psychiatric disorders, and other symptoms are brought on by the degeneration of these areas. Therefore, it is essential to recognize changes in these areas early on in order to intervene and manage effectively.

In the early stages of AD, various medicinal strategies can reduce symptoms. Diagnostic evaluations frequently include brain imaging, mental health assessments, neurological tests, physical examinations, and studies of medical histories [4]. Specifically, brain imaging allows for the non-invasive viewing of the structure, function, as well as pharmacology of the brain [5]. Due to its lack of radiation and lack of invasiveness, MRI has become the gold standard among neuroimaging techniques [6]. But traditional MRI scans only pick up on the brain's structure, so they may overlook the functional alterations brought on by AD.

There are two main kinds of MRI: structural (sMRI) as well as functional (fMRI). SMRI documents the anatomy of brain structures, revealing their size and shape, whereas fMRI evaluates brain activity by identifying changes in blood flow, allowing visualization of neural responses to stimuli or activities [7]. In recent years, multi-modal MRI, which combines both sMRI and fMRI, has gained attention for providing complementary structural and functional insights into brain alterations related to Alzheimer’s disease. However, manual interpretation of these images are more time-consuming and may result in inconsistent or biased interpretations. Hence, there is a pressing need for automated techniques to efficiently predict AD.

Recent advancements in Artificial Intelligence (AI) have provided promising tools to aid physicians in identifying and localizing early AD markers [8]. Researchers are able to identify subtle early indicators of AD, often prior to the emergence of clinical symptoms, by analyzing these MRI scans using sophisticated AI algorithms. The possibility for multi-modal diagnosis is enhanced by these models' ability to detect complex patterns that may indicate the development of AD [9, 10]. DL along with Machine Learning (ML) are two main categories of AI. ML techniques have been applied to enhance diagnostic procedures by analyzing and interpreting complex neuroimaging data. Models like Support Vector Machines (SVM) [11], Random Forest (RF) [12], and k-Nearest Neighbors (k-NN) [13] have been widely used in AD diagnosis because to their ability to learn from labeled data and spot trends. However, these models require manual feature engineering and can be hindered by the high dimensionality of multi-modal neuroimaging data.

Received: August 04, 2025

International Journal of Applied Mathematics
Volume 38 No. 12s 2025,
ISSN: 1311-1728 (printed version); ISSN: 1314-8060 (on-line version)

In contrast, DL techniques have been addressed these limitations by automatically feature representations directly from raw imaging data. Several DL based methods like Recurrent Neural Networks (RNNs) [15], Long Short-Term Memory (LSTMs) [16], Convolutional NN (CNNs) [14], as well as Deep Belief Networks (DBNs) [17] are the DL models applied for AD detection. Various DL models have been developed for AD prediction. For instances, DenseNet-121 with LeNet and AlexNet were combined in parallel to perform AD detection faster [18]. In this approach, a trio of tiny filters stand in the traditional array of huge convolutional filters. However, this model suffered from the gradient losses. ResNet-50 model was used for AD detection using MRI of the brain [19]. However, one disadvantage of using ResNet is the potential disappearance of gradients in very deep networks, which can make the gradient descent process slow. Ensemble Convolutional Neural Networks (ECNN) [20] was developed using Line Segment Feature Analysis (LFA), VGGnet and 1DCNN model for AD classification based on the brain's structure. LFA retrieves the important morphological features, VGGnet model derived global biomarkers from raw MRI data. An improved method for detecting AD using vectors signals from visual information was to extract local biomarkers using a 1DCNN. The LFA data in the ensemble CNN model, on the other hand, focuses solely on object shape features, which can cause performance issues if other feature information is ignored. Also, MRI just refers to the general structure of the brain, it alone cannot provide full efficiency on examining AD.

1.1 Major Contributions

Therefore, in this research, a novel multimodal framework called Enhanced Ensemble Brain Connected AD Network (EEBCADnet) is introduced for accurate as well as reliable categorization of AD stages. Unlike existing methods that rely on a single imaging modality, EEBCADnet effectively combines fMRI and sMRI data to capture both neural activity and anatomical alterations. The model fuses graph-theoretical connectivity measures, deep CNN-based representations, and Refined Local Feature Analysis (LFA) features, providing a comprehensive and discriminative understanding of AD-related brain changes. The main achievements are these:

- Initially, a robust pre-processing structure is introduced to refine fMRI, T1-weighted, and T2-weighted scans. The processed fMRI data are then parcellated using the Glasser atlas, dividing the cortex into 360 functionally homogeneous Regions Of Interest (ROIs).
- In the second stage, the coefficient of correlation of the time series among ROIs is used to estimate the edge weight, which involves creating an adjacency matrix with each brain region serving as a node. Then, binary and weighted functional connectivity matrices are produced.
- Third, in order to quantitatively represent the topological structure of the brain's functional network, a graph-theoretical extraction of features module calculates local as well as global network measures.

Received: August 04, 2025

ISSN: 1311-1728 (printed version); ISSN: 1314-8060 (on-line version)

- Fourth, a multilevel feature fusion strategy integrates graph-theoretical features with deep features and Refined Line Feature Analysis (LFA)–derived structural features such as feature points and line segments. This multimodal fusion enables a rich and complementary representation of both global connectivity and fine structural information.
- The fifth step in the EEBCADnet classification module's process for making probabilistic predictions between AD stages is the use of a FC layer next to a softmax layer.
- Finally, the proposed EEBCADnet framework demonstrates strong predictive performance on benchmark datasets, highlighting its ability to jointly leverage functional connectivity and structural representations for accurate and interpretable AD prediction.

The proposed EEBCADnet framework thus brings together multimodal learning, graph-based analysis, and deep feature fusion to form a powerful and stable system for AD classification. The remainder of the paper is organized as follows: The study is set up as follows: A review of pertinent studies is given in Section 2, the methodology is described in Section 3, the results are presented and discussed in Section 4, and the research is concluded with a discussion of possible extensions in Section 5.

2. LITERATURE SURVEY

Houria et al. [21] introduced a multimodal MRI fusion framework that integrates diffusion tensor imaging (DTI) and sMRI to enhance the early diagnosis of AD. The method captures white matter (WM) microstructural alterations using DTI-derived scalar metrics and detects gray matter (GM) atrophy over sMRI. After features were extracted from both modalities using a Two-Dimensional CNN (2D-CNN), an SVM was used to categorize the combined data.

Jia & Lao [22] devised a multi-modal AD prediction framework. Before applying the mean Regional Homogeneity (mReHo) conversion to the fMRI data, the sMRI as well as fMRI scans were preprocessed. Feature extraction was then performed using 3DMR-PCANet for the mReHo images and a 3DResNet-10 model, built using stacked ResNet modules, for the sMRI scans. For the final classification, a SVM classifier was employed after the retrieved multimodal features were fused utilizing Kernel Canonical Correlation Analysis (KCCA). However, the sensitivity and specificity values are degraded due to the complete dependence on handcrafted feature extraction.

Long et al. [23] presented a multi-modal MRI analysis framework in which metrics from resting-state fMRI as well as sMRI were extracted and analyzed. The AAL3 atlas was used to determine the Hurst Exponent (HE), bilateral hippocampal seed-based connectivity and Gray Matter Volume (GMV) for each region of interest using fMRI and sMRI, respectively. To achieve feature selection, a Sequential Feature Collection (SFC) method was used together with Minimal Redundancy Maximal Relevance (MRMR) to save just the most relevant

Received: August 04, 2025

International Journal of Applied Mathematics
Volume 38 No. 12s 2025,
ISSN: 1311-1728 (printed version); ISSN: 1314-8060 (on-line version)

features. Lastly, to distinguish between AD, MCI, as well as Healthy classes, SVM and ANN classifiers were used. However, the model resulted in poor accuracy due to limited dataset.

A hybrid DL framework that incorporates neuropsychological test data with MRI and PET scans was proposed by Hassan et al. [24] for the purpose of early AD identification. The approach takes use of a CNN when combined with a LSTM network to record temporal and spatial characteristics. A deep CNN model was also employed for multi-stage AD classification, while transfer learning with pretrained weights and image entropy selection was used to improve performance with limited data. However, the classifiers utilize longer computation times because of its complexity.

Baniata et al. [25] established a DL-based MAGNet for AD classification using sMRI, fMRI, and PET scans. The model used a multi-modal attention method to capture both global and fine-grained properties by hierarchically fusing information from multiple modalities. MAGNet incorporated multi-task learning with auxiliary tasks to enhance feature generalization. An interpretability module generates attention maps highlighting brain regions influential for classification decisions. But, this model failed to balance the accuracy across all classes.

For the purpose of detecting AD in small-sample multi-modal imaging data, Liu et al. [26] developed the Cross-Scale Equilibrium Pyramid Coupling (CSEPC) framework. In order to obtain balanced multiscale characteristics from both sMRI along with fMRI, the approach integrates them utilizing a cross-scale pyramid module. After that, a cosine similarity coupling technique based on contrastive learning is employed to fuse these features. This reduces the number of learning variables while efficiently capturing inter- and intra-modal associations. However, pre-processing steps of fMRI data were complex which may increase its computation time and memory.

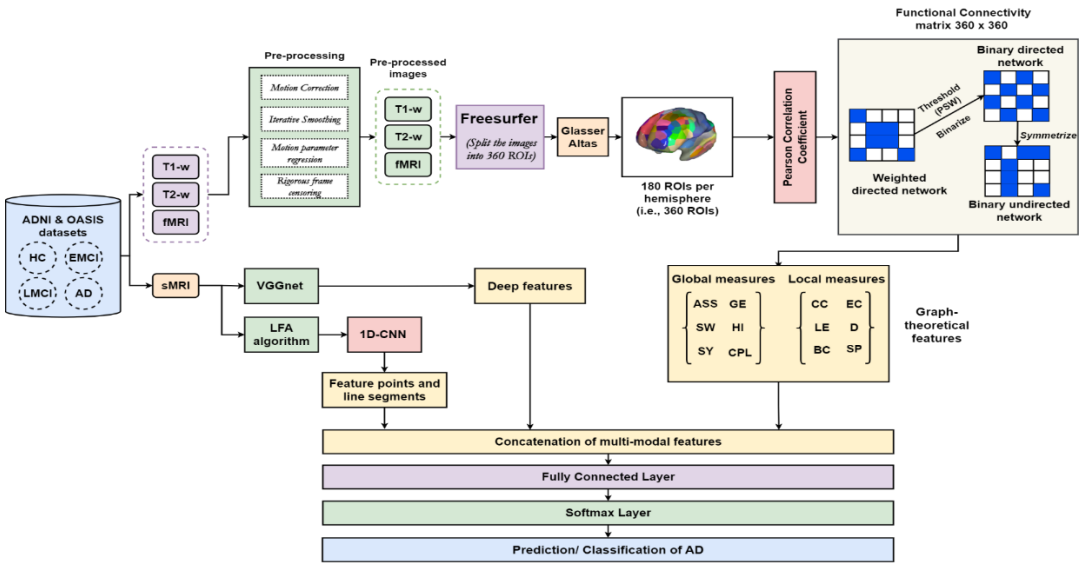

Figure 1. Pipeline of the Proposed Method

Received: August 04, 2025

International Journal of Applied Mathematics
Volume 38 No. 12s 2025,
ISSN: 1311-1728 (printed version); ISSN: 1314-8060 (on-line version)

3. PROPOSED METHODOLOGY

Figure 1 depicts the suggested EEBCADnet model, which is described in this section.

3.1 Overview of EEBCADnet

This study develops an EEBCADnet to predict and classify AD progression by unifying functional and structural feature representations. The methodology is primarily grounded on fMRI analysis where inter-regional relationships are modelled to construct an adjacency matrix which captures connectivity patterns. Along with fMRI, T1-weighted and T2-weighted MRi are also considered to include the information that are not given in structural MRIs. This gives network features of fMRI, combining both global and local measures. The structural features like deep features (extracted by VGGNet), line segments and feature points (extracted by 1D-CNN and LFA) [20] complement the functional network, thereby resulting in multi-modal feature representations for AD prediction. The subsequent sections will explain each steps involve in the proposed AD prediction model.

3.2 Data pre-processing

The fMRI data, T1- and T2-weighted structural images, are first carefully pre-processed to ensure high data quality and to reduce artifacts caused by differences in image acquisition. This preprocessing pipeline typically includes motion correction, nuisance regression, frame censoring, and spatial smoothing [27]. Motion correction is used to estimate and compensate for head movement that occurs between scans. It involves calculating rigid-body movement parameters for each frame and then realigning the time series of brain images accordingly. After this step, nuisance regression is performed to further reduce motion-related noise by including the six estimated motion parameters as regressors in a statistical model. Frame censoring is then applied to remove time points that are heavily affected by motion. Frames that exceed a predefined movement threshold, often based on metrics such as Framewise Displacement (FD) are excluded to avoid introducing motion artifacts into subsequent analyses. Finally, spatial smoothing is applied before computing functional connectivity networks. In this step, the signal at each voxel is averaged with the signals from its neighbouring voxels using a smoothing kernel, which helps to enhance the signal clarity ratio as well as promotes comparability across participants.

3.3 FreeSurfer for Brain Segmentation and surface reconstruction

Once the preprocessed images are obtained, FreeSurfer is employed to perform volumetric segmentation and surface reconstruction. Neuroimaging data can be analyzed with the use of FreeSurfer, a suite of tools that offers a variety of methods to measure the brain's structural, functional, and connectional features. From creating mostly cortical surface models, it has progressed to automatically creating models of the majority of the major macroscopic brain regions from any appropriate T1-weighted image. Being open source and publicly available, it is compatible with many different computer systems and software programs. Based on intensity differences in the image (e.g., white matter is brighter than gray matter), FreeSurfer segments

International Journal of Applied Mathematics
Volume 38 No. 12s 2025,
ISSN: 1311-1728 (printed version); ISSN: 1314-8060 (on-line version)

the brain volume. This includes labelling subcortical structures and creating a white matter mask. A rough surface mesh is created from the white matter segmentation volume. The mesh is then fine-tuned by shifting its vertices to form a "white surface" that corresponds more closely to the intensity gradients among the gray as well as white matter. The white surface is expanded outward along intensity gradients to form a pial surface, which marks the boundary between gray matter and cerebrospinal fluid (CSF). This vertex-specific cortical thickness is measured by the white-pial surface distance.

3.4 Parcellation using Glasser Atlas

The cerebral cortex is then divided into 360 Regions of Interest (ROIs), or 180 ROIs for each hemisphere. Glasser atlas is applied. Using a variety of multi-modal data, such as topographical organization, connection patterns, and architectural information from T1w/T2w imaging and fMRI, it uses a gradient-based cortical parcellation technique. The atlas provides incredibly accurate cortical area delineation by combining these many data sources. Additionally, co-localized gradient ridges across modalities are used to identify initial areal borders, guaranteeing a strong, data-driven, but expert-validated mapping procedure. In conclusion, it separates the cerebral cortex into 180 ROIs each hemisphere, or 360 ROIs total. Individual participants can be precisely aligned because each ROI represents a unique cortical area with shared anatomical and functional characteristics. The binary brain connectivity matrix and the weighted brain connection matrix are then created using the covariance factors of all the fMRI data from these 360 regions.

3.5 Functional Connectivity Matrix Construction

Every brain region identified by the Glasser atlas is a node in the functional brain network. The correlation coefficient between the fMRI time series of any two brain regions represents the edge weight connecting the corresponding nodes. This approach results in a 360 × 360 adjacency matrix for each subject, where each matrix component represents the degree of functional relationship between two places. To eliminate self-connections, the diagonal elements are set to zero. The Proportion of Strong Weights (PSW) thresholding approach, which successfully suppresses noise and weak correlations, is then used to produce both weighted and binary adjacency matrices. This data-driven method maximizes the network's Global Cost Efficiency (GCE), which is determined by

$$max_{PSW}(GCE) = E - PSW \quad (1)$$

$$E = \frac{1}{n}\sum_{i\in N} E_i = \frac{1}{n}\sum_{i\in N} \frac{\sum_{j\in N, j\neq i} d_{ij}^{-1}}{n-1} \quad (2)$$

where n is the total amount of nodes, N is the vector of all nodes, d_{ij} is the shortest path length between nodes i and j and E_i is the efficiency of node i.

where n represents the overall number of vertices, N denotes the set of all vertices, d_{ij} is the minimum distance between vertex i and j and E_i refers to the performance (or effectiveness)

Received: August 04, 2025

International Journal of Applied Mathematics
Volume 38 No. 12s 2025,
ISSN: 1311-1728 (printed version); ISSN: 1314-8060 (on-line version)

of vertex i. Once the strongest weight ratio has been determined, a sparse brain connection matrix is produced. By assessing absolute correlation values and keeping only undirected functional linkages between cortical regions, negative correlations are eliminated. Lastly, the weighted network and the binary undirected network are both maintained.

3.6 Global and local measures using Graph theory

The structural features of the brain's functional network are measured using graph-theoretical analysis after weighted a

nd binary adjacency matrices have been established. Each node (brain region) and edge (functional connection) contribute to the overall network architecture, capturing both local efficiency of individual regions and global integration across the entire brain. For each subject, there are set of network measures computed from both matrix types. These are categorized as 6 global and 6 local measures. Assortativity (ASS), Global Efficiency (GE), Hierarchy (HI), Synchronization (SY), Small World (SW) and Characteristic path length (CPL) are characteristics for the global measurements. Furthermore, clustering coefficient (CC), Local Efficiency (LC), Between centrality (BC), Eigenvector Centrality (EC), Degree (D) and Shortest Path (SP) are among the 360 properties of each local measure in the binary network.

Assortativity: It is the co-variance factor between each node's degree on a pair of opposing connection endpoints. It is more probable for nodes with a positive assortativity coefficient to establish connections with nodes of comparable or equal degree.

Global efficiency: The global efficiency of the network is its average inverse shortest path length.

Small world: It measures a network's small-world characteristic, which combines short average path lengths with high local clustering.

Characteristic path length (CPL): It defines the network’s mean shortest path length.

Clustering coefficient: The clustering coefficient equivalent to the fraction of neighbors who are neighbors of one another, is the percentage of triangles that surround a node.

Local efficiency: It is correlated with the clustering coefficient and is the global efficiency calculated on adjacent nodes.

Betweenness centrality: The percentage of the network's shortest paths that contain a specific node is known as node betweenness centrality. Numerous shortest pathways involve nodes with high betweenness centrality scores.

Eigenvector centrality: Nodes with high eigenvector centrality are those that connect to other nodes with high eigenvector centrality. Eigenvector centrality is a self-referential measure of centrality.

Received: August 04, 2025

International Journal of Applied Mathematics
Volume 38 No. 12s 2025,
ISSN: 1311-1728 (printed version); ISSN: 1314-8060 (on-line version)

Degree: The amount of links that are attached to a node is known as its node degree. The number of inward and outward nodes which are known to be in and out -degree, respectively with directed networks. The calculations do not take connection weights into account.

These features are combined for each subject to form the final feature vector, which has 2,166 measurements (6 global measures and 6 × 360 local measures). All metrics are normalized to [−1, 1] prior to additional analysis.Since they offer quantifiable measurements of the structural and functional alterations in the AD brain network, these metrics are crucial for the fMRI classification of AD.

3.7 Structural features

Since this study focuses on multimodal neuroimaging data, the structural MRI (sMRI) data are analyzed in conjunction with the fMRI data. Two categories of structural features are extracted from the sMRI scans: deep features and geometric features based on Line-segment Analysis (LFA). Deep features capture high-level structural characteristics of brain anatomy, including complex shape, texture, and spatial organization across cortical and subcortical regions. These representations are automatically learned rather than manually defined, allowing the model to encode subtle morphological differences. In this work, deep features are extracted using a pre-trained CNN called VGGNet. The VGGNet architecture is a deep, layered network known for its strong performance. It relies on a series of 3×3 convolutional filters, and its variants like VGG16 and VGG19 are distinguished by their total number of layers. Generally, increasing the number of layers in this model leads to enhanced overall performance.

In contrast, geometric features provide interpretable structural features derived from Line Feature Analysis (LFA). Line segments are treated by LFA as basic geometric primitives that characterize the local structural organization of the brain. The LFA approach uses pixel-level line segments to represent object outlines, transforming visual data into structured data. It determines the most common line features in the image by examining the kinds and frequencies of these segments.

A 1D-CNN architecture, which learns discriminative patterns from the ordered line-segment feature sequences, is used to model these line features. Prior to training the 1D CNN model, 1D input is converted using the LFA approach. Since the altered data were created by removing visual characteristics, a comprehensive examination of all the data was pointless. Nonetheless, important aspects might be gleaned from the condensed data if the variations in the coefficients for every kind of line segment were investigated. In the converted data, change linkages between successive values similar to those in time-series data are especially important. Consequently, these features were extracted using the 1D CNN model. This model consists of ten parallel layers. Additionally, $Z_{i.k}^{n}$ feature map of Conv-n is calculated with n^{th} convolution layer of the 1D CNN of i^{th} output neuron value, using the following formula $Z_{i.k}^{n} = b_k^n + \sum_{u=0}^{f_s^n-1}\sum_{k'=0}^{f_m^n-1} x_{i'k'}.W_{u,k}^{n}$ (3)

Received: August 04, 2025

International Journal of Applied Mathematics
Volume 38 No. 12s 2025,
ISSN: 1311-1728 (printed version); ISSN: 1314-8060 (on-line version)

where $x_{i'k'}$ indicates the final value of the i' location in the k feature map of the preceding layer and b_k^n represents bias term. Since there is only one layer in this 1D CNN, using padding is pointless. To gather the strongest features among the output features, the global max-pooling function is also used to the forecast the output devised by the 1D convolution layer.

3.8 Concatenation of multi modal features

Once the graph-theoretical measures were obtained, a final feature vector was constructed using concatenation approach. This vector combines the functional connectivity features from both global and local measures of fMRI, each contributing 2,166 features per subject. To further enrich this representation, two additional approaches were incorporated in this study (as mentioned in the previous section).

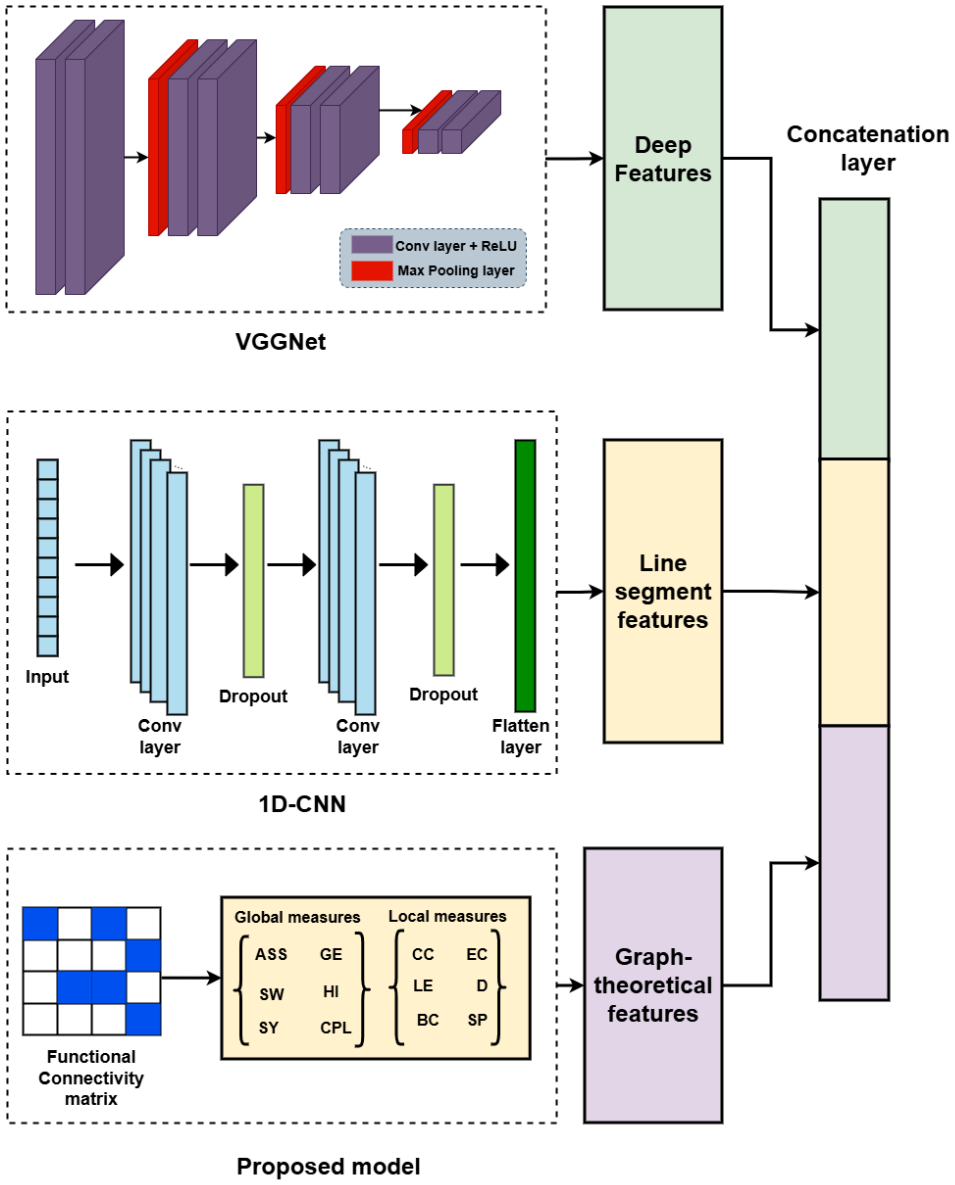

Figure 2. Concatenation of multi-modal features

Received: August 04, 2025

ISSN: 1311-1728 (printed version); ISSN: 1314-8060 (on-line version)

First, a VGGNet was used to retrieve the deep features straight from the raw MRI data because graph-theoretical measures only capture manufactured characteristics. Second, while graph-theoretical measures summarize inter-regional relationships, they do not explicitly encode feature points or cortical outlines, which may lead to performance degradation when image resolution or size varies. To address this, an LFA analysis was applied to 1DCNN which then extracts key feature points and line segment features, from each subject's brain.

Finally, a final fused feature vector is produced by integrating these graph-theoretical features, deep features and LFA-derived feature points and line segments. This fused feature vector is then transmitted to the fully connected layer, which analyzes the retrieved features to discover global patterns associated with AD. It allows the model to integrate both data and generate the final feature vector by connecting each neuron to all of the outputs from the preceding layer. Figure 2 shows the pipeline for concatenating these features.

3.9 Classification

The final stage of the proposed EEBCADnet model is to classify the final feature vector obtained from the previous fusion stage. For this, a softmax function is used to convert the network's output into a probabilistic distribution across target classes. During training, the network is optimized using a cross-entropy loss function, ensuring that the predicted probability approximately corresponds to the ground-truth labels.

4. RESULT AND DISCUSSION

The evaluation of the proposed model is presented in this part to show its effectiveness.

4.1 Dataset Description

1) Alzheimer's Disease Neuroimaging Initiative (ADNI) dataset [29]: The information included in this study came from a reputable and openly accessible source for AD research. The early detection and progression of Alzheimer's disease at various stages have been thoroughly studied using this dataset. The dataset contains numerous modalities, however only two are investigated in this study: sMRI and fMRI. A comprehensive description of the dataset is provided in Table 1.

Table 1. Comphrensive overview of the ADNI Dataset

Scrutiny	Number of Records
Mild Cognitive Impairment	3924
Alzheimer's Disease	1731
Cognitively Normal	2665
Total	**8320**

Received: August 04, 2025

ISSN: 1311-1728 (printed version); ISSN: 1314-8060 (on-line version)

Also, the dataset contains longitudinal data, with multiple visits per participant recorded at intervals ranging from 0 to 120 months (July 2005 to May 2017). Each participant has 502 attributes, including demographic information (e.g., age, gender), cognitive assessments (e.g., Mini-Mental State Examination (MMSE) scores), and neuroimaging scans. Notably, the MMSE score serves as a key parameter for assessing cognitive decline: lower scores indicate greater impairment, which is crucial for labeling and evaluating disease progression in this dataset.

2) Open Access Series of Imaging Studies-3 (OASIS-3) dataset [30]: Second, the OASIS-3 dataset, which is a retrospective collection of data from 1,378 people gathered over a 30-year period through several research carried out by the WUSTL Knight AD Research Center (ADRC). Participants in the sample range in age from 42 to 95 years, and there are 622 people in different stages of cognitive impairment in addition to 755 adults who are cognitively normal. Multiple imaging modalities, including T1-weighted (T1w), T2-weighted (T2w), FLAIR, arterial spin labeling (ASL), susceptibility-weighted imaging (SWI), time-of-flight (TOF), resting-state BOLD (fMRI), and diffusion tensor imaging (DTI) sequences, are included in the 2842 MRI sessions that make up OASIS-3. Volumetric segmentation files derived from FreeSurfer are included with several of these sessions. The collection also includes post-processed outputs produced by the PET Unified Pipeline (PUP) including PET imaging data with many tracers, such as PIB, AV45, FDG, and Tau (AV1451). In this investigation, which examined the structural and functional alterations in the brain associated with the progression of AD, only the sMRI and fMRI modalities were included for analysis.

4.2 Performance Metrics

The metrics used to assess both the current and proposed models are illustrated below.

1. Accuracy: It evaluates a model's overall accuracy by calculating the proportion of correctly classified samples to the total number of samples.

$$Accuracy = \frac{TP+TN}{TP+FP+TN+FN} \tag{16}$$

where TP, TN, FP, and FN represent True Positives, True Negatives, False Positives, and False Negatives, respectively.

2. Precision: It denotes the fraction of accurately predicted positive instances among all instances anticipated as positive. It demonstrates the accuracy of the model's positive forecasts.

$$Precision = \frac{TP}{TP+FP} \tag{17}$$

3. Sensitivity: It evaluates how well the model can distinguish between all true positives and positive cases. There are fewer false negatives when the sensitivity is increased.

Received: August 04, 2025

International Journal of Applied Mathematics
Volume 38 No. 12s 2025,
ISSN: 1311-1728 (printed version); ISSN: 1314-8060 (on-line version)

$$Sensitivity = \frac{TP}{TP+FN} \quad (18)$$

4. F1-score: It provides a balanced statistic that takes into consideration both false-positive and false-negative errors by representing the harmonic mean of precision and recall. When working with datasets that have unequal class distributions, this metric is quite helpful.

$$F1 - score = 2 \times \frac{Precision \times Sensitivity}{Precision + Sensitivity} \quad (19)$$

5. Specificity: It evaluates how effectively the model recognizes true negative cases among all actual negatives. Also, it reflects the model's capability to minimize false-positive evaluations.

$$Specificity = \frac{TN}{TN+FP} \quad (20)$$

4.3 Performance Assessment

By contrasting the suggested model with other models such as CNN [24], SVM-ANN [23], 2DCNN-SVM [21], CSEPC [26], and MAGNet [25], this section evaluates the overall effectiveness of the model.

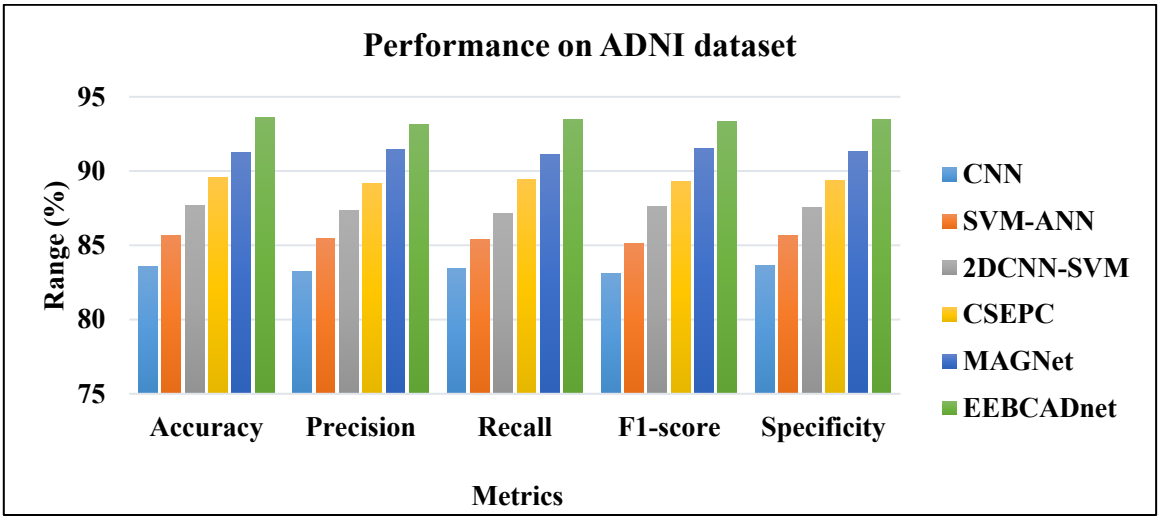

Figure 2. Evaluation of suggested and existing models on ADNI dataset

Figure 2 summarizes the performance comparison of several models on the ADNI dataset, including CNN, SVM-ANN, 2DCNN-SVM, CSEPC, MAGNet and the suggested EEBCADnet. The suggested EEBCADnet model demonstrated its better capacity to correctly categorize AD phases by achieving the highest performance across all evaluation metrics. In particular, EEBCADnet outperformed CNN, SVM-ANN, 2DCNN-SVM, CSEPC, and MAGNet by 12.0%, 8.9%, 6.7%, 4.5%, and 2.6%, respectively. In a similar vein, the precision and recall figures show notable improvements of roughly 11–12% over CNN and roughly 2–5% over the most recent models. Additionally, the F1-score significantly improved, indicating

Received: August 04, 2025

International Journal of Applied Mathematics
Volume 38 No. 12s 2025,
ISSN: 1311-1728 (printed version); ISSN: 1314-8060 (on-line version)

a better balance between recall and precision. Additionally, the specificity demonstrates that EEBCADnet successfully separates AD with less FPs.

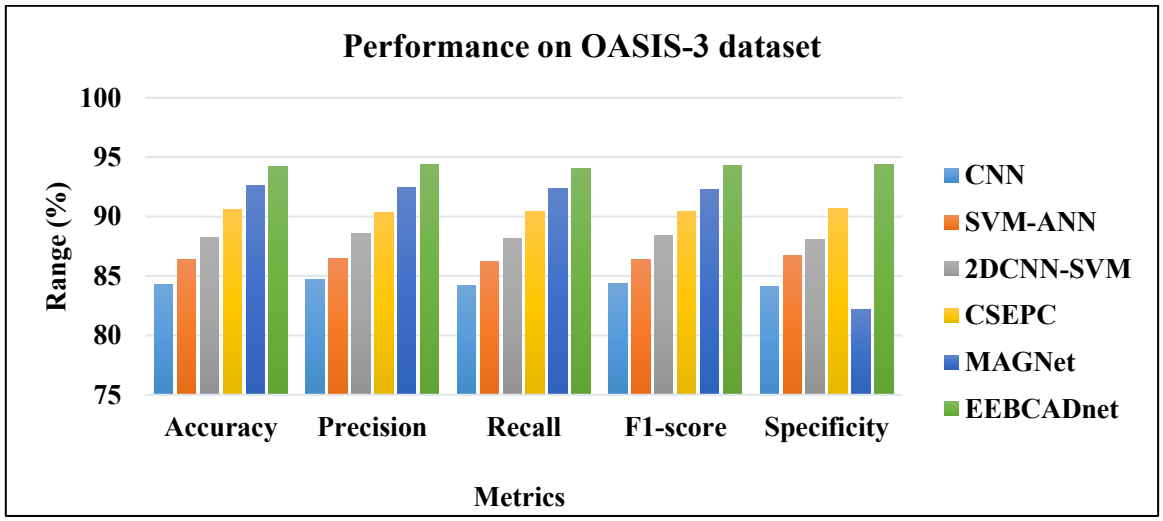

Figure 3. Performance Evaluation of proposed and existing models on OASIS-3 dataset

The performance comparison of various models including CNN, SVM-ANN, 2DCNN-SVM, CSEPC, MAGNet, and the proposed EEBCADnet on the OASIS-3 dataset is summarized in Figure 3. The suggested EEBCADnet model demonstrated its better capacity to correctly categorize AD phases by achieving the highest performance across all evaluation metrics. In particular, EEBCADnet outperformed CNN, SVM-ANN, 2DCNN-SVM, CSEPC, and MAGNet by 11.8%, 8.4%, 6.0%, 4.0%, and 1.7%, respectively. Comparably, the precision and recall numbers show notable improvements of roughly 10–12% over CNN and 2-4 percent over the most recent models currently in use. Additionally, the F1-score significantly improved, indicating a better balance between recall and precision. Additionally, the specificity demonstrates that EEBCADnet successfully separates AD with less FPs.

4.4 Statistical Validation

In scientific research, particularly in medical imaging, the process of validating a proposed model extends beyond achieving high accuracy, it requires statistically confirming that the observed improvements did not occurred by chance. This logical foundation mirrors the core principles of hypothesis testing in inferential statistics. Hypothesis testing allows researchers to thoroughly assess if the performance of the suggested EEBCADnet model indeed constitutes a substantial improvement over current approaches in this AD detection study.

While the null hypothesis (H_0) assumes that there is no appreciable difference in classification performance between the proposed and existing models, the alternative hypothesis (H_1) argues that the suggested model achieves actually improved performance due to its enhanced learning and feature fusion mechanisms. To validate this claim, statistical hypothesis testing is employed to establish whether the accuracy gains are mathematically relevant at a predefined confidence level (often $p < 0.05$). To achieve this, the paired t-test is executed to statistically

Received: August 04, 2025

International Journal of Applied Mathematics
Volume 38 No. 12s 2025,
ISSN: 1311-1728 (printed version); ISSN: 1314-8060 (on-line version)

assess whether the mean performance difference between EEBCADnet and existing models is significant, thereby reinforcing the robustness of the proposed approach.

Table 2. Paired t-test validation for proposed and existing models in terms of accuracy

Model	t-value	df	Sig. (2-tailed)	Mean Difference (%)	Std. Dev	95% Confidence Interval	
						Lower	Upper
ADNI Dataset							
CNN	8	4	0.001	10.01	2.8	6.54	13.48
SVM-ANN	6.82	4	0.002	7.89	2.59	4.68	11.1
2DCNN-SVM	4.64	4	0.01	5.9	2.84	2.37	9.43
CSEPC	3.88	4	0.018	4.02	2.32	1.14	6.9
MAGNet	5.16	4	0.007	2.33	1.01	1.08	3.58
OASIS-3 Dataset							
CNN	8.15	4	0.001	9.92	2.72	6.54	13.3
SVM-ANN	6.58	4	0.002	7.87	2.68	4.55	11.19
2DCNN-SVM	4.43	4	0.011	5.97	3.02	2.23	9.71
CSEPC	3.55	4	0.022	3.65	2.3	0.79	6.51
MAGNet	3.84	4	0.018	1.65	0.96	0.46	2.84

The results of the paired t-test comparing the suggested EEBCADnet model with the present models for categorizing AD on the ADNI and OASIS-3 datasets are shown in Table 2. Each model's t-value, degrees of freedom, standard deviation, mean accuracy difference, 2-tailed significance (p-value), and 95% confidence range are all included. In this instance, the recommended EEBCADnet model serves as the reference model. The fact that every p-value is less than 0.05 suggests that the advancements made by EEBCADnet are statistically significant and can't have happened by chance. The mean differences, along with their confidence intervals, highlight the magnitude and reliability of these improvements, demonstrating that EEBCADnet consistently outperforms existing methods across both datasets.

5. CONCLUSION

To categorize AD phases, this study suggested an EEBCADnet framework based on DL. By integrating sMRI and fMRI data, the model captures both anatomical and functional alterations in the brain. The framework combines graph-theoretical connectivity measures, CNN-based deep features, and RLFA features. Experimental evaluation on two benchmark datasets, ADNI and OASIS-3, demonstrated that EEBCADnet consistently outperforms existing methods, including CNN, SVM-ANN, 2DCNN-SVM, CSEPC, and MAGNet, achieving accuracies of 93.58% and 94.23%, respectively. These enhancements are statistically significant, according

Received: August 04, 2025

ISSN: 1311-1728 (printed version); ISSN: 1314-8060 (on-line version)

to paired samples t-test analysis, which highlights the approach's resilience and reliability. Future studies could look into popular optimization strategies to further enhance the model's performance and efficiency across a range of datasets and architectures.

REFERENCES

[1] Tiwari, S., Atluri, V., Kaushik, A., Yndart, A., & Nair, M. (2019). Alzheimer's disease: pathogenesis, diagnostics, and therapeutics. International journal of nanomedicine, 5541-5554.

[2] World Health Organization. Dementia: a public health priority. Geneva: World Health Organization; 2012.

[3] Sridhar, S., Khamaj, A., & Asthana, M. K. (2023). Cognitive neuroscience perspective on memory: overview and summary. Frontiers in Human Neuroscience, 17, 1217093.

[4] Frisoni, G. B. (2001). Structural imaging in the clinical diagnosis of Alzheimer's disease: problems and tools. Journal of Neurology, Neurosurgery & Psychiatry, 70(6), 711-718.

[5] Yen, C., Lin, C. L., & Chiang, M. C. (2023). Exploring the frontiers of neuroimaging: a review of recent advances in understanding brain functioning and disorders. Life, 13(7), 1472.

[6] Sedgwick, A. C., Brewster, J. T., Harvey, P., Iovan, D. A., Smith, G., He, X. P., ... & James, T. D. (2020). Metal-based imaging agents: progress towards interrogating neurodegenerative disease. Chemical Society Reviews, 49(10), 2886-2915.

[7] Hojjati, S. H., Ebrahimzadeh, A., & Babajani-Feremi, A. (2019). Identification of the early stage of Alzheimer's disease using structural MRI and resting-state fMRI. Frontiers in neurology, 10, 904.

[8] Vrahatis, A. G., Skolariki, K., Krokidis, M. G., Lazaros, K., Exarchos, T. P., & Vlamos, P. (2023). Revolutionizing the early detection of Alzheimer's disease through non-invasive biomarkers: the role of artificial intelligence and deep learning. Sensors, 23(9), 4184.

[9] Venugopalan, J., Tong, L., Hassanzadeh, H. R., & Wang, M. D. (2021). Multimodal deep learning models for early detection of Alzheimer's disease stage. Scientific reports, 11(1), 3254.

[10] Zhang, F., Li, Z., Zhang, B., Du, H., Wang, B., & Zhang, X. (2019). Multi-modal deep learning model for auxiliary diagnosis of Alzheimer's disease. Neurocomputing, 361, 185-195.

[11] NP, K. T., & Varghese, D. (2018, May). A Novel Approach for Diagnosing Alzheimer's Disease Using SVM. In 2018 2nd International Conference on Trends in Electronics and Informatics (ICOEI) (pp. 895-898). IEEE.

[12] Saied, I. M., Arslan, T., & Chandran, S. (2021). Classification of Alzheimer's disease using RF signals and machine learning. IEEE Journal of Electromagnetics, RF and Microwaves in Medicine and Biology, 6(1), 77-85.

[13] Aruchamy, S., Mounya, V., & Verma, A. (2020, December). Alzheimer's disease classification in brain MRI using modified kNN algorithm. In 2020 IEEE international

ISSN: 1311-1728 (printed version); ISSN: 1314-8060 (on-line version)

symposium on sustainable energy, signal processing and cyber security (iSSSC) (pp. 1-6). IEEE.

[14] AbdulAzeem, Y., Bahgat, W. M., & Badawy, M. (2021). A CNN based framework for classification of Alzheimer's disease. Neural Computing and Applications, 33(16), 10415-10428.

[15] Cui, R., Liu, M., & Alzheimer's Disease Neuroimaging Initiative. (2019). RNN-based longitudinal analysis for diagnosis of Alzheimer's disease. Computerized Medical Imaging and Graphics, 73, 1-10.

[16] Hong, X., Lin, R., Yang, C., Zeng, N., Cai, C., Gou, J., & Yang, J. (2019). Predicting Alzheimer's disease using LSTM. Ieee Access, 7, 80893-80901.

[17] Xia, Z., Zhou, T., Mamoon, S., & Lu, J. (2021). Recognition of dementia biomarkers with deep finer-DBN. IEEE Transactions on Neural Systems and Rehabilitation Engineering, 29, 1926-1935.

[18] Hazarika, R. A., Maji, A. K., Kandar, D., Jasinska, E., Krejci, P., Leonowicz, Z., & Jasinski, M. (2023). An approach for classification of Alzheimer's disease using deep neural network and brain magnetic resonance imaging (MRI). Electronics, 12(3), 676.

[19] Nithya, V. P., Mohanasundaram, N., & Santhosh, R. (2024). An early detection and classification of Alzheimer's disease framework based on ResNet-50. Current Medical Imaging, 20(1), e250823220361.

[20] Kim, C. M., & Lee, W. (2023). Classification of Alzheimer's disease using Ensemble Convolutional Neural Network with LFA Algorithm. IEEE Access.

[21] Houria, L., Belkhamsa, N., Cherfa, A., & Cherfa, Y. (2022). Multi-modality MRI for Alzheimer's disease detection using deep learning. Physical and Engineering Sciences in Medicine, 45(4), 1043-1053.

[22] Jia, H., & Lao, H. (2022). Deep learning and multimodal feature fusion for the aided diagnosis of Alzheimer's disease. Neural Computing and Applications, 34(22), 19585-19598.

[23] Long, Z., Li, J., Fan, J., Li, B., Du, Y., Qiu, S., ... & Jing, B. (2023). Identifying Alzheimer's disease and mild cognitive impairment with atlas-based multi-modal metrics. Frontiers in Aging Neuroscience, 15, 1212275.

[24] Hassan, A., Imran, A., Yasin, A. U., Waqas, M. A., & Fazal, R. (2024). A Multimodal Approach for Alzheimer's Disease Detection and Classification Using Deep Learning. Journal of Computing & Biomedical Informatics, 6(02), 441-450.

[25] Baniata, M., Abuowaida, S., Aljaidi, M., Kharabsheh, M., Alsarhan, A., & Alsuwaylimi, A. A. (2025). A Multi-Modal Attention-Guided Network for Alzheimer's Disease Classification Using Deep Learning. Engineering, Technology & Applied Science Research, 15(5), 27150-27158.

[26] Liu, J., Yu, X., Fukuyama, H., Murai, T., Wu, J., Li, Q., & Zhang, Z. (2025). CSEPC: a deep learning framework for classifying small-sample multimodal medical image data in Alzheimer's disease. BMC geriatrics, 25(1), 130.

Received: August 04, 2025

ISSN: 1311-1728 (printed version); ISSN: 1314-8060 (on-line version)

[27] Zhang, A., Pagliaccio, D., Marsh, R., & Lee, S. (2022). Decoding age-specific changes in brain functional connectivity using a sliding-window based clustering method. bioRxiv, 2022-09.

[28] Glasser, M. F., Coalson, T. S., Robinson, E. C., Hacker, C. D., Harwell, J., Yacoub, E., ... & Van Essen, D. C. (2016). A multi-modal parcellation of human cerebral cortex. *Nature*, *536*(7615), 171-178.

[29] https://adni.loni.usc.edu/

[30] https://sites.wustl.edu/oasisbrains/home/oasis-3/

Received: August 04, 2025